

## Model and Control of Novel Surface-Motor in Plane Motion

Liu Xuepeng, Mei Xuesong, Wu Xutang

### Abstract:

Model of the novel Surface motor (SFM) is briefly discussed, and two types of control method including two-order feedback circuit control, indirect acceleration feedback control are analyzed to solve unstable characteristic such as low damp and negative stiffness. The simulation results demonstrate that the system has plain amplitude and wide frequency band arranging from 0 to 8kHz with no resonant peak through indirect acceleration feedback control.

### 1. Introduction

Surface motor (SFM), also named planar motor, utilizes electromagnetic force to achieve high precision motor without friction. The surface motor driven system (SFM) based on electromagnetic technology is superior to other traditional system due to the frictionless, nanometer resolution, 6-DOF movement and lighter weight. The surface-motor driven stage attracts more and more attention.

Many research centers are involved in the development of surface motors usually based on Sawyer motor topology which enables bi-directional motion using one motor and reported upon its basic structure and specifications<sup>[1][2][3][4][5][6][7]</sup>, some students are concerned about Bi-directional Magnetic Microactuator<sup>[8]</sup>. Here, however, this novel surface motor presented has quite different characteristics: a stationary slotless armature with orthogonal windings and a mover with air bearing.

The novel surface motor control problem is low damp and negative stiffness due to the inherent unstabilities associated with the electro-mechanical dynamics. Besides, the SFM has a narrow frequency band and resonant peak. Therefore, the controller to be developed should work in stable condition with large range frequency. The conventional control

---

**Keywords:** surface motor; plane motion; electromagnetic field; PID; indirect acceleration feedback.

scheme is proportional-differential strategy. However, this scheme can enlarge the noise of signal data. Therefore, this paper focuses on the proportional-integral-differential control with two-stage feedback because it can meet the requirement of stable condition.

This paper presents an improved strategy for controlling the SFM system.

The organization of this paper is as follows. Section 1 describes the design aspects of the prototype system proposed here, and provides a detailed mathematic model. In Section 2, a proportional-integral-differential controller for the prototype SFM system is presented, which can achieve the stable condition for positioning. Besides, an indirect acceleration feedback is attained for decreasing the noise in the signal. Simulation results demonstrate the effectiveness. Finally, conclusions are drawn in Section 3.

## 2. Basic principle of the SFM

Figure 1 presents the perspective view of the surface motor stage; the stage has a stator with a plane surface and a mover with four air bearings. It has a multiphase armature windings wound round with an iron plate. Every phase is produced in such a way: one winding is assembled round the x-axis forming the x-coil sections, and the other round the y-axis forming the y-coil sections. The orthogonal windings have no electric connections one with the other and are assembled in intercalated layers. There are 16 independent coil sections or phases. Each one has 200 turns. The plate is 180mm wide, 180mm long and 10mm thick. Between the mover and the stator there are four air bearings and four solenoids, the former give the horizontal force to support the mover, while the latter provide the force to move the mover. A PWM driver is used to feed the independent coil sections of multiphase windings in a switching mode fashion. Only the necessary coil sections will be excited simultaneously. The coil section under solenoids is excited before the mover is coming toward the exciting coil section, then next coil section is excited. The moving direction is parallel to plane surface. Based on the structure, the mover can move step by step<sup>[9]</sup>.

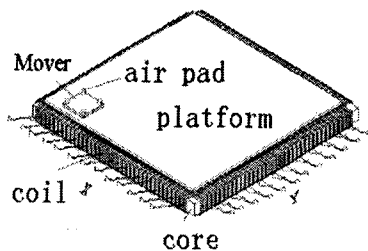


Fig.1 structure of SFM

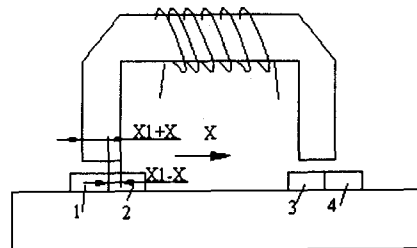


Fig.2 lateral force

Figure 2 presents a schematic frontal section of the stage. When the NO 1 coil is excited by differential current  $I$  and the bias current  $i$ , the NO 2 coil by differential current  $-I$  and the bias current  $i$ , the solenoids of the mover can create force on two coils that pushes or pull it accordingly. Since the different direction current the force on NO 1 coil is opposite to that on NO 2 coil. The resolution of the stage can be obtained by the control of the bias current  $i$ . According to magnetic circuit principle, taking into consideration that the magnetic resistance of the air is much larger than that of the iron, the magnetic pressure falls on the air gap. The magnetic density can be obtained by the following:

$$N_d I_d = \oint H dl \quad (1)$$

In equation (1),  $N_d$  is the turn of each phase,  $I_d$  is the current of solenoid, and  $l$  is length of the magnetic circuit. The magnetic field is given by:

$$B = \mu_0 \times H = \mu_0 \times \frac{N_d I_d}{2h} \quad (2)$$

where  $\mu_0$  is permeability of the air,  $h$  is the height of the air gap. The magnetic force can be obtained by applying Ampere's law:

$$F = \int Idl \times B \quad (3)$$

$$F = \int (I_1 + i) dl \times B - \int (I_1 - i) dl \times B \quad (4)$$

The formula  $\int (I_1 + i) dl \times B$  and  $\int (I_1 - i) dl \times B$  represents the force of the NO 1 coil and the NO 2 coil. The current is even distributed along the X-axis and Y-axis. One derives:

$$I(x) = \frac{x}{w} \times i \quad (5)$$

The symbol  $w$  is the width of the phase. By using equations (4) and equation (5), it gives:

$$\begin{aligned} F &= \frac{(x_1 + x)}{w} (I_1 + i) \times Bl - \frac{(x_1 - x)}{w} (I_1 - i) \times Bl \\ &= \frac{(2xI_1 + 2x_1i)}{w} \times Bl \\ &= K_i i + K_x x \end{aligned} \quad (6)$$

in equation (6),  $K_i$  is the current gain of the stage,  $x_1 = w/2$ .

$$K_i = \frac{2x_1}{w} \times Bl \quad (7)$$

$K_x$  is negative magnetic stiffness,

$$K_x = \frac{2 I_1}{w} \times Bl \quad (8)$$

From the equation (6), the force is connected not only with exciting current but also with the displacement of the mover. The characteristic of the driving force is opposite to that of the spring, which stays away from the stable point. So it is the unstable factor.

The equation of the dynamic model of stage is:

$$m \ddot{x} + b \dot{x} = 4F \quad (9)$$

where  $b$  is the damp,  $m$  is the mass, and  $4F$  is the force of four solenoids. Combing the equation (8) with equation (9) gives the following equation:

$$m \ddot{x} - 4K_x x + b \dot{x} = 4K_i i \quad (10)$$

By means of Laplace transform, then we obtain:

$$\frac{x(s)}{i(s)} = \frac{4K_i}{ms^2 + bs - 4K_x} \quad (11)$$

According to equation (9), equation (10) and equation (11), it is concluded:

(1). Since the damp is nearly zero, the model is lack of damp, which makes the stage oscillate.

(2). The magnetic stiffness is called as "negative stiffness", which tries to make the stage unstable.

### 3. The method of control

Assuming the inductance and the resistance of the every phase is  $R, L$ . The electric equation is:

$$U = iR + L \frac{di}{dt} \quad (12)$$

After Laplace transform, the electric equation is in form of:

$$\frac{i(s)}{U(s)} = \frac{1}{R + Ls} \quad (13)$$

Combining the equation (11) and the equation (13), we obtain:

$$\begin{aligned} \frac{x(s)}{U(s)} &= \frac{4K_i}{(ms^2 + bs - 4K_x)(R + Ls)} \\ &= \frac{4K_i}{K_3 s^3 + K_2 s^2 + K_1 s + K_0} \end{aligned} \quad (14)$$

In equation (14),  $K_3 = mL$ ,

$$K_2 = mR + bL,$$

$$K_0 = -4K_x R$$

$$K_1 = bR - 4K_x L.$$

The design aim of the analog inner loop is to make the system stable in order to get suitable damp by using the characteristic of good real-time ability of analogical calibration. Proportion-differential Cascade compensator is often utilized in second-order system with lack of damp and negative stiffness. Schematic diagram of closed control loop is shown in Fig. 3 by using the PD control.

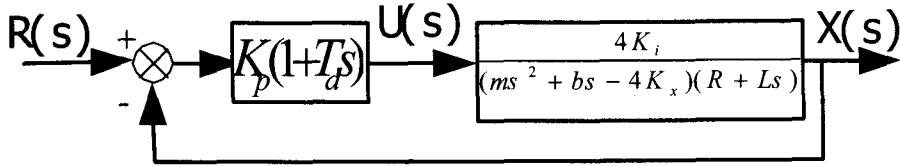


Fig.3 PD control diagram

The transfer transform of the closed loop control system is:

$$G(s) = \frac{K_p(1 + T_d s) \times 4K_i K_w}{K_3 s^3 + K_2 s^2 + (K_1 + K_{pd} T_d) s + K_{pd} + K_0} \quad (15)$$

where  $K_{pd} = 4K_i K_p$

Obviously, only two of four characteristic polynomial coefficients can be regulated for third-order closed-loop transfer function by means of adjusting the parameter  $K_p, T_d$ , which can't control the pole of the complex plane efficiently. So it is limited to improve the ability of system by proportion-differential control.

In this paper, a two-stage feedback is presented, which is position feedback and

acceleration feedback. Combining the two-stage feedback with PID control controls the analogical inner loop. The schematic of the principle is shown in Fig.4.

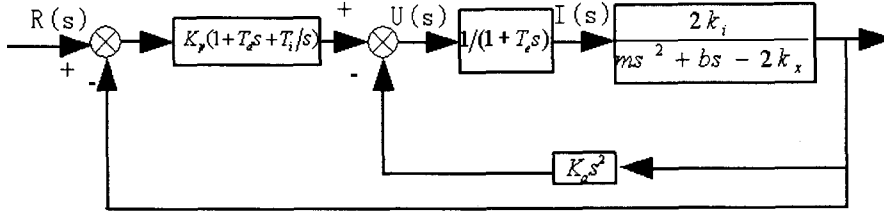


Fig.4 PID control diagram

In Fig.4,  $T_d, T_i, K_p$  is differential coefficient, integration coefficient, proportional coefficient,  $K_a$  is acceleration constant, the other parameters are defined before. The transform function of the closed-loop is:

$$G(s) = \frac{4K_{sum}(1 + T_d s + T_i/s)}{Lms^4 + K_{s3}s^3 + K_{s2}s^2 + K_{s1}s + 4K_{sum}} \quad (16)$$

where  $K_{sum} = K_i K_p$

$$K_{s3} = bL + mr + 4K_i K_a$$

$$K_{s2} = (-4K_x L + br + 4K_{sum} T_d)$$

$$K_{s1} = -4K_x r + 4K_{sum} \quad (17)$$

In terms of Routh stability criterion, the condition of stable closed-loop is:

$$\begin{cases} b_1 = K_{s3} \times K_{s2} - L \times m \times K_{s1} > 0 \\ a_1 = K_{s1} > 0 \\ a_3 = K_{s3} > 0 \end{cases} \quad (18)$$

From the equation (18), the system can be on stable condition if  $T_d$  and  $K_p$  is large enough, which can be easily realized.

After analyzing the transform function of the PID acceleration feedback and its

characteristic polynomial, four of five characteristic polynomials can be adjusted by controlling the PID parameters and acceleration parameter logically, which means that the position of pole can be easily adjusted everywhere in theory. So the performance of the

closed-loop system, including lacking damp, can be enhanced. The step response is shown in Fig.5.

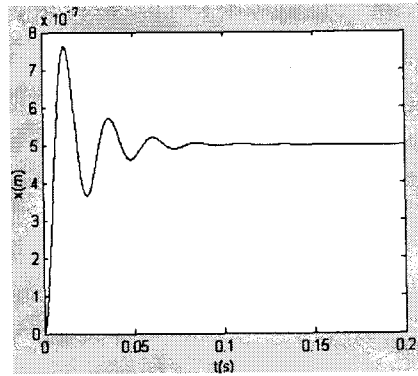


Fig.5 step of PID control

In Fig.5, the blue curve represents the step response. From the curve, we can draw a conclusion: it takes 0.1s to achieve the stable condition. The parameters used in Fig.5 are listed below:

$$\begin{aligned} T_d &= 0.2; \\ K_p &= 8.8e5; \\ T_i &= 0.01; \\ K_a &= 100. \end{aligned}$$

The transfer function can be reduced to two-stage system in order to analyze the analogical closed-loop transfer function easily, which is:

$$G(s) = \frac{0.013286 (s + 1.332 \times 10^8)}{(s^2 + 1008s + 1.764 \times 10^6)} \quad (19)$$

The bode diagram of closed-loop system is shown in Fig.6

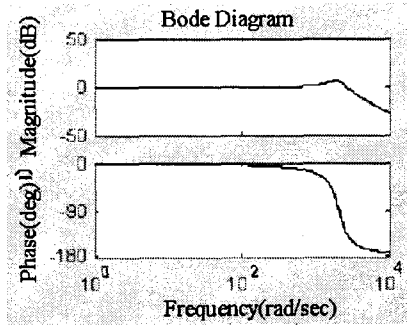


Fig.6 bode diagram of PID control

From Fig.6, the system has the plain amplitude-frequency characteristic, wide frequency band, which provides a good base for next digital outer control so as to obtain high precision. However, the system has the resonant peak. A new method is put forward.

One of main merits of surface motor is to move without friction or without contact. In this field, displacement, speed and acceleration without sensor is one important research. In this paper, a new method is issued to obtain the signal. In theory, a second order differential of displacement is equal to obtain the sign of acceleration. There is a certain noise in feedback signal in displacement sensor for a general control system, which can be magnified through the differential algorithm. The differential circuit may cause phase delay over high frequency, so a method to obtain the acceleration indirectly is presented based on the driving principle of Surface motor. One formula can be derived from equation (10).

$$\ddot{x} = \frac{4K_i i + 4K_x x - bx}{m} \quad (20)$$

Since the value of  $b$  is small, the damp can be ignored, and then equation (20) can be simplified as:

$$\ddot{x} = f_i i + f_x x \quad (21)$$

where  $f_i = \frac{4K_i}{m}$



$$f_x = \frac{4 K_x}{m} \tag{22}$$

The interferometer can obtain high resolution<sup>[10]</sup>, so the signal of displacement can be obtained through the laser interferometer and the signal of the current through the current sensor. The proportional algorithm circuit is designed to obtain equivalent signal of

acceleration according to the equation (20). The block diagram by using equivalent acceleration feedback is shown in Fig.7.

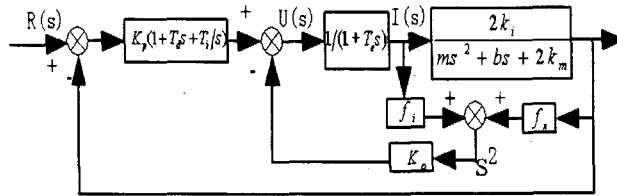


Fig.7. Schematic diagram

The simulation result of system by no acceleration sensor feedback is shown in Fig.8. From the Fig.8 we conclude: It takes 10ms to achieve the stable condition.

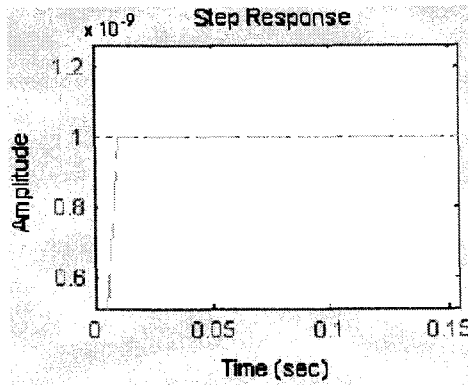


Fig.8 step response

The bode diagram by no acceleration feedback is shown in Fig.9, a conclusion is drawn: The system has plainer amplitude-frequency and wider frequency band characteristic by

using no-acceleration sensor than by using two-stage differential circuit. The system has no resonant peak.

The transfer function can be reduced to second-order system in order to analyze the analogical closed-loop transfer function easily, which is:

$$G(s) = \frac{453.0689(s + 238.9)}{(s^2 + 464.3s + 1.115 \times 10^5)} \quad (23)$$

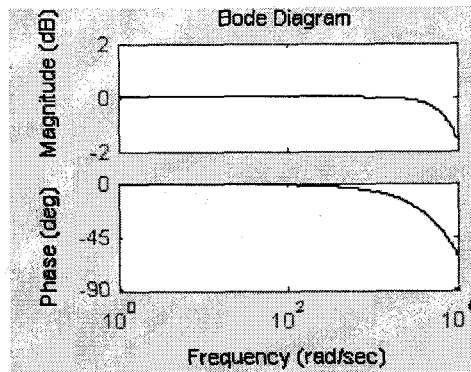


Fig.9 bode diagram

#### 4. Conclusion

This project is on research for next generation manufacture technology on the premise that there are some achievements about Surface motor. A model of analogical inner closed-loop is established on the base of Surface motor's driving principle. This paper presents a PID and two-stage feedback control method. The system has plain amplitude-frequency characteristic, wide frequency band and suitable damp. However, second-order differential enlarges the noise in high frequency and phase delay in fact; a control method with no acceleration sensor is presented. The result of simulation demonstrates that the performance can be improved to achieve the predicted aim by this method.

#### 5. Acknowledgments

This project is supported by National Nature Science Foundation (NO 50275117).

#### Reference

1. D.Ebihara, T.Watanobe and M.Watada. "Characteristics Analysis of Surface Motor",

2. IEEE Transaction on Magnetics, 1992, 28(5): 3033~3035.
3. A.E.Brennemann and R.L.Hollis. "Magnetic and Optical-Fluorescence Position Sensing for Planar Linear Motor", Proc. Of the 1995 IEEE/RSJ Int. Conf. On Intelligent Robots and Systems, 1995, vol.3.101-107.
4. Tomita.Y, Koyanagawa.Y and Sotah.F, "A Surface Motor-Driven Precision Positioning System", Precision Engineering. 1994. 16(3): 184~191.
5. D.Ebihara, and M.Watada. "The Study on Basic Structure of Surface Actuator", IEEE Transaction on Magnetic. 1989.25(5): 3916~3918.
6. Won-Jong Kim and D.L.Trumper, "High-precision magnetic levitation stage for photolithography", Precision Engineering, 1998.22(2):66;
7. Tomita.Y, Koyanagawa.Y and Sotah.F, "A Surface Motor-Driven Precision Positioning System", Precision Engineering. 1994.16(3):184~191.
8. D.Ebihara, T.Watanobe and M.Watada, "Characteristics Analysis of Surface Motor", IEEE Trans on Magnetics. 1992.28(5):3033~3035.
9. H. J. Cho and C. H. Ahn, "A Bi-directional Magnetic Microactuator Using Electroplated Permanent Magnet Arrays", IEEE Journal of Microelectromechanical Systems (JMEMS), pp. 78-84, Vol. 11, No. 1, 2002
10. A.F.Flores Filho, A.A.Susin, M.A.da Silveira, "Development of A Novel Planar Actuator", Ninth International Conference on Electrical Machine and Drive. 1991, NO.468:268-271.
11. M.Sasaki, X.Mi, K.Hane "Standing wave detection and interferometer application using photodiode thinner than optical wavelength" Appl. Phys. Lett., 75, pp.2008-2011, 1999

Xi'an Jiaotong University,  
Xi'an 710049,China